FINAL REPORT

Advanced Ocean Surface Measurements with HF Radar

University of Michigan Project
031605

Office of Naval Research Grant:
N00014-94-1-0371

Prof. John F. Vesecky, Principal Investigator

Atmospheric, Oceanic and Space Science Dept.
The University of Michigan

February, 1997

REPORT DOCUMENTATION PAGE

Form Approved
OMB No. 0704-0188

[illegible]

1. AGENCY USE ONLY (Leave blank)	2. REPORT DATE	3. REPORT TYPE AND DATES COVERED
	January, 1997	Technical Report, 1/1/94-12/31/95

4. TITLE AND SUBTITLE
Advanced Ocean Surface Measurements with HF ~~Ground~~ Wave Radar

5. FUNDING NUMBERS
N00014-94-1-0371

6. AUTHOR(S)
John F. Vesecky, Calvin C. Teague, Robert G. Onstott, and Peter E. Hansen

7. PERFORMING ORGANIZATION NAME(S) AND ADDRESS(ES)
Atmospheric, Oceanic, and Space Sciences Dept.
The University of Michigan
2455 Hayward St.
Ann Arbor, MI 48109-2143

8. PERFORMING ORGANIZATION REPORT NUMBER
031605-97-1-

9. SPONSORING/MONITORING AGENCY NAME(S) AND ADDRESS(ES)
Office of Naval Research

10. SPONSORING/MONITORING AGENCY REPORT NUMBER

11. SUPPLEMENTARY NOTES

12a. DISTRIBUTION/AVAILABILITY STATEMENT
Unlimited

12b. DISTRIBUTION CODE

13. ABSTRACT *(Maximum 200 words)*

HF surface wave radar for ocean wave and current measurements began with collaborative work at Stanford University and Scripps Institution of Oceanography in the late 1960's. Two of the participants in this project (Drs. Teague and Vesecky) have worked with HF radar observations of the ocean since these early experiments. Under this grant a new HF radar design was begun and some prototype construction completed. This work led to construction of a full scale prototype that is now being tested over Monterey Bay, California from a field site kindly provided at the Long Marine Laboratory of the University of California at Santa Cruz. Initial results, including radial current field maps at four frequencies and variations of currents with time, were presented at the American Geophysical Union Fall Meeting in San Francisco, December, 1996. This final report is a presentation of results under the funding from ONR grant N00014-94-1-0371. It contains an overview of the radar design and its implementation in hardware as well as some preliminary results on vertical shear in the surface current field over Monterey Bay CA.

14. SUBJECT TERMS
HF Radar, Ocean Currents, Current Shear, Coastal Oceanography

15. NUMBER OF PAGES
47

16. PRICE CODE

17. SECURITY CLASSIFICATION OF REPORT	18. SECURITY CLASSIFICATION OF THIS PAGE	19. SECURITY CLASSIFICATION OF ABSTRACT	20. LIMITATION OF ABSTRACT
UNC	UNC	UNC	Unlimited

NSN 7540-01-280-5500

Standard Form 298 (Rev 2-89)
Prescribed by ANSI Std Z39-18
298-102

Introduction and Abstract

HF surface wave radar for ocean wave and current measurements began with collaborative work at Stanford University and Scripps Institution of Oceanography in the late 1960's. This work at Stanford was largely funded by ONR from about 1970 to 1980. Two of the participants in this project (Drs. Teague and Vesecky) have worked with HF radar observations of the ocean since these early experiments. Since that time, HF radar as an ocean sensing tool has progressed with increasing acceptance in the oceanography community over the last five years. A research project to design and build an advanced, multifrequency HF radar began in 1992 with seed money from the University of Michigan and the Environmental Research Institute of Michigan (ERIM). This early phase was followed by a cooperative effort involving Michigan, Stanford and ERIM. This final report presents the results early ONR funding from the remote sensing core area. During this period a new HF radar design was begun and some prototype construction completed. This work led to construction of a full scale prototype that is now being tested over Monterey Bay, California from a field site kindly provided at the Long Marine Laboratory of the University of California at Santa Cruz. This operation is in collaboration with the REINAS project at UC Santa Cruz that is also funded by ONR. Prof. Pat Mantey and Dr. Dan Fernandez of UC Santa Cruz provided much help during the Santa Cruz operations and the results of the radar measurements are being made available over the internet by the REINAS project. A second radar unit is nearing completion and will be integrated and deployed in June 1997. Initial results, including radial current field maps at four frequencies and variations of currents with time, were presented at the American Geophysical Union Fall Meeting in San Francisco, December, 1996. Although these experimental results were obtained on later ONR grants we present them here to show the fruition of the early work funded under this initial ONR grant.

This final report is a presentation of results under the funding from ONR grant N00014-94-1-0371. It contains an overview of the radar design and its implementation in hardware as well as some preliminary results. The success of this early phase of the research project came through the efforts of participants at several institutions working in close collaboration, as follows:

University of Michigan
- Prof. John Vesecky, principle investigator
- Peter Hansen, project engineer
- Dr. Jason Daida, software development and data analysis
- Neil Schnepf, graduate student
- Ray Pung, undergraduate research assistant

Stanford University
- Dr. Calvin Teague and Prof. Len Tyler

Environmental Research Institute of Michigan (now ERIM International)
- Dr. Robert Onstott
- Dr. Robert Shuchman
- Dr. Ken Fischer

Finally the strong support and excellent suggestions from Drs. Dennis Trizna and Frank Herr at the Office of Naval Research are important in the present and future success of the project.

I. Radar Design Summary

The radar design is summarized in the block diagram of Fig. 1. It incorporates a number of novel features and many improvements relative to previous HF radar designs. The radar is completely under computer control so that flexible remote operation is possible. The current unit, now at the Long Marine Laboratory of the University of California at Santa Cruz (LML) is operated remotely by logging into the control computer over the internet. The radar currently operates on four frequencies to give measurements of currents at effective depths of from 30 cm below the surface down to about 1.6 meters. Thus, shear in this largely unknown region can be explored and air-sea interaction better understood. The radar uses a pseudo random coded waveform and pulse compression to improve signal to noise ratio relative to simple pulse systems. We think that this type of waveform will allow higher power operation as the potential interference with other users of the HF spectrum will be reduced. These features should lead to larger ranges -- our current goal is a reliable range of 100 km with a transmitter input power of 500 to 1000 watts.

We will now discuss some of the hardware aspects of the system. As shown in Fig. 1, the radar consists of a pulse modulated transmitter, two vertical transmitting antennas, an array of electronically switched receiving loop antennas, and a specialized linear HF receiver, all under computer control. The transmitter is direct-sequence modulated with a pseudo-random pulse train generating a spread-spectrum signal. The transmitter carrier frequency is also rapidly changed (or hopped) among four different values between 4 and 25 MHz. The pseudo-noise or PN code sequence (called the chipping sequence) is also used by the receiver to coherently detect the return pulse train containing the Doppler information.

Transmitter and Transmit Antennas: The transmitter contains a phase stable reference oscillator used for both transmit carrier synthesis and receiver local oscillator injection. The 80 MHz reference carrier is applied to a direct digital synthesizer or DDS. Under computer control, the synthesizer generates any carrier frequency in the HF spectrum, but in our specific application only four FCC approved frequencies are used. The synthesized carrier is applied to a balanced mixer for amplitude modulation by the computer generated PN code discussed earlier. The resulting signal is then applied to two identical solid state amplifier chains, one for the low band signals (4 to 8 MHz), and one for the high band signals (8 to 25 MHz). Each of the two transmit chains has its own 1/4 wave vertical antenna and counterpoise. Each vertical antenna is resonant at two of the frequencies of interest. The transmitter power output is $\approx$150 watts PEP with capability to add linear amplifiers at a later date.

Receive Antennas: The receive antenna array consists of 8 non-resonant square loops constructed out of ordinary copper pipe supported with PVC plumbing fittings. The spectra from each antenna are coherently added in the computer after the phase is adjusted in order to steer the antenna array main beam direction. Each loop

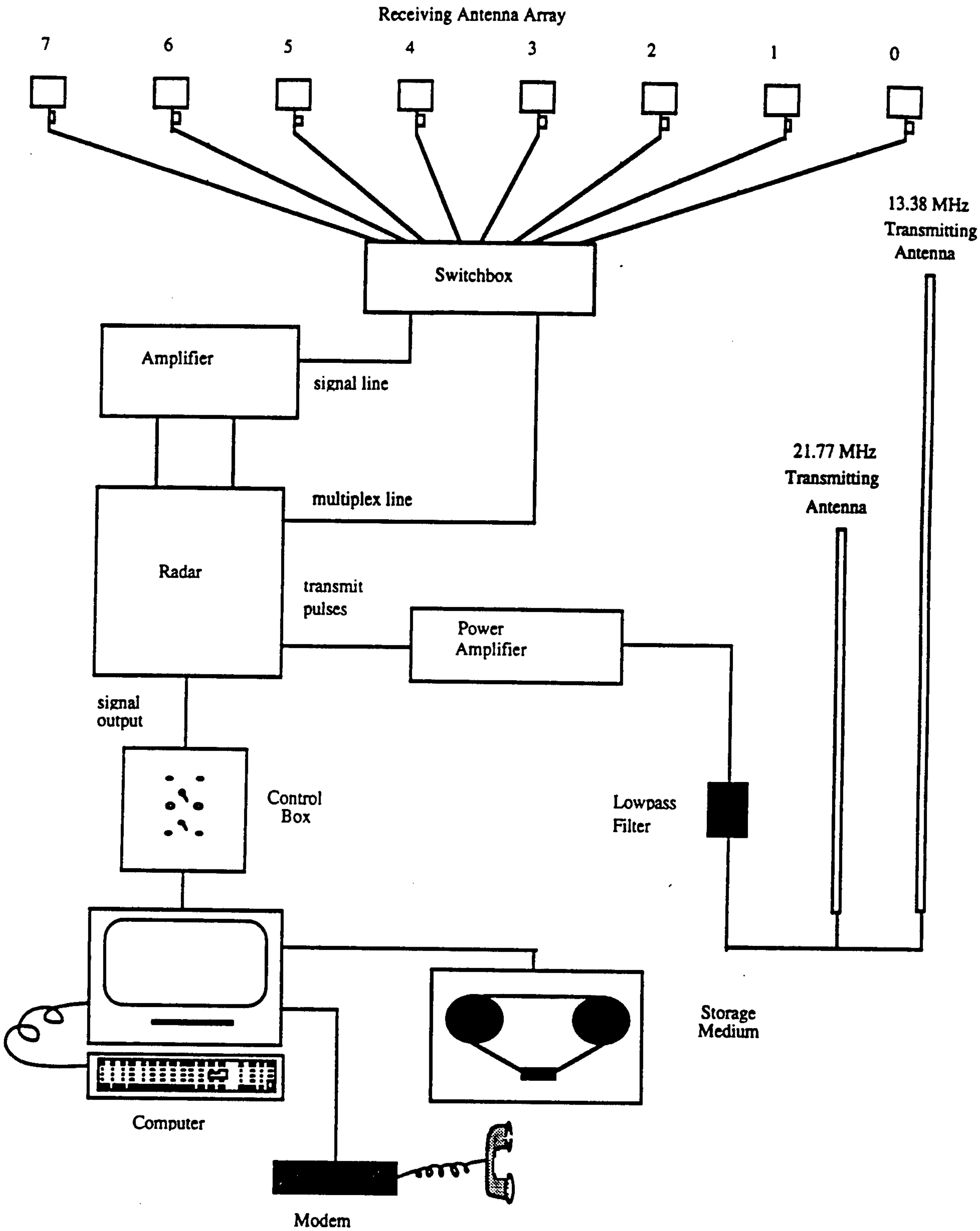

Fig. 1. HF radar system block diagram

is 2.5 ft on a side as dictated by what one gets when cutting a standard 10 foot length of copper pipe into four pieces. Built into the bottom section of the antenna support pipe is a preamplifier containing a blanker circuit to disable the receiver input during the radar transmit pulse time, preventing receiver overload. This blanker functions the same as the pulse blankers in most modern receivers, except that it is done right at the antenna input, rather than at the receiver IF frequency. The preamplifier also includes a bandpass filter to reject out of band signals. Each receive antenna preamplifier output is applied to a solid state electronic 8 by 1 multiplexer controlled by the computer.

Receiver: The receiver is a single conversion design having a computer controlled RF preselector, computer controlled IF gain, and computer controlled post detection bandwidth. The IF is at 40 MHz having a bandwidth of 200 kHz. Phase linearity is an important parameter for the design of the receiver, and considerable attention has been given to the IF filtering in order to provide good phase linearity. Receiver gain is controlled by adjusting an electronic attenuator in the IF amplifier section. This attenuator consists of a set of biased diodes driven by a computer controlled D/A converter. The detection circuit consists of two identical phase detectors driven by in-phase and quadrature 40 MHz reference signals. Both an in-phase and quadrature phase comparison of the radar return signal is required in order to distinguish positive and negative frequencies resulting from approaching and receding ocean waves. The post detection filtering is performed by switched capacitor low pass filters under computer control. The two detected analog baseband signals are sampled and converted to digital information by two identical 12 bit A/D converters.

Controller: The system controller is a microcontroller board having a 68332 processor with 256K of RAM. External to this board are auxiliary interface circuits consisting of several PALs, a serial communications controller (SCC), RS422 line drivers, a background interface and 12 bit D/A and A/D converters. The SCC is used to route the receiver digital data to a Macintosh 7100/66 computer (Power MAC) used for the data analysis. Macintosh-based C/C++ compilers by Metrowerks are used to generate code.

II. Radar Equipment Construction

A single radar is designed to fit in an ECS composite shock mounted cabinet about 3 ft. tall with a 2 x 2 ft. footprint -- see Fig. 2. The cabinet has detachable wheels and can be used as a shipping container for the radar. The control computer, currently a Macintosh Power PC 7100/60, is connected to the radar by several cables. The equipment is mounted within the enclosure in 19" rack panel chassis containing the following (with numbers according to Fig. 2):

2. Spare rack for future needs
3. Radar controller and exciter chassis
4. Radar receiver chassis
5. Radar transmitter chassis
10. Power supplies
6. Mains power control panel.

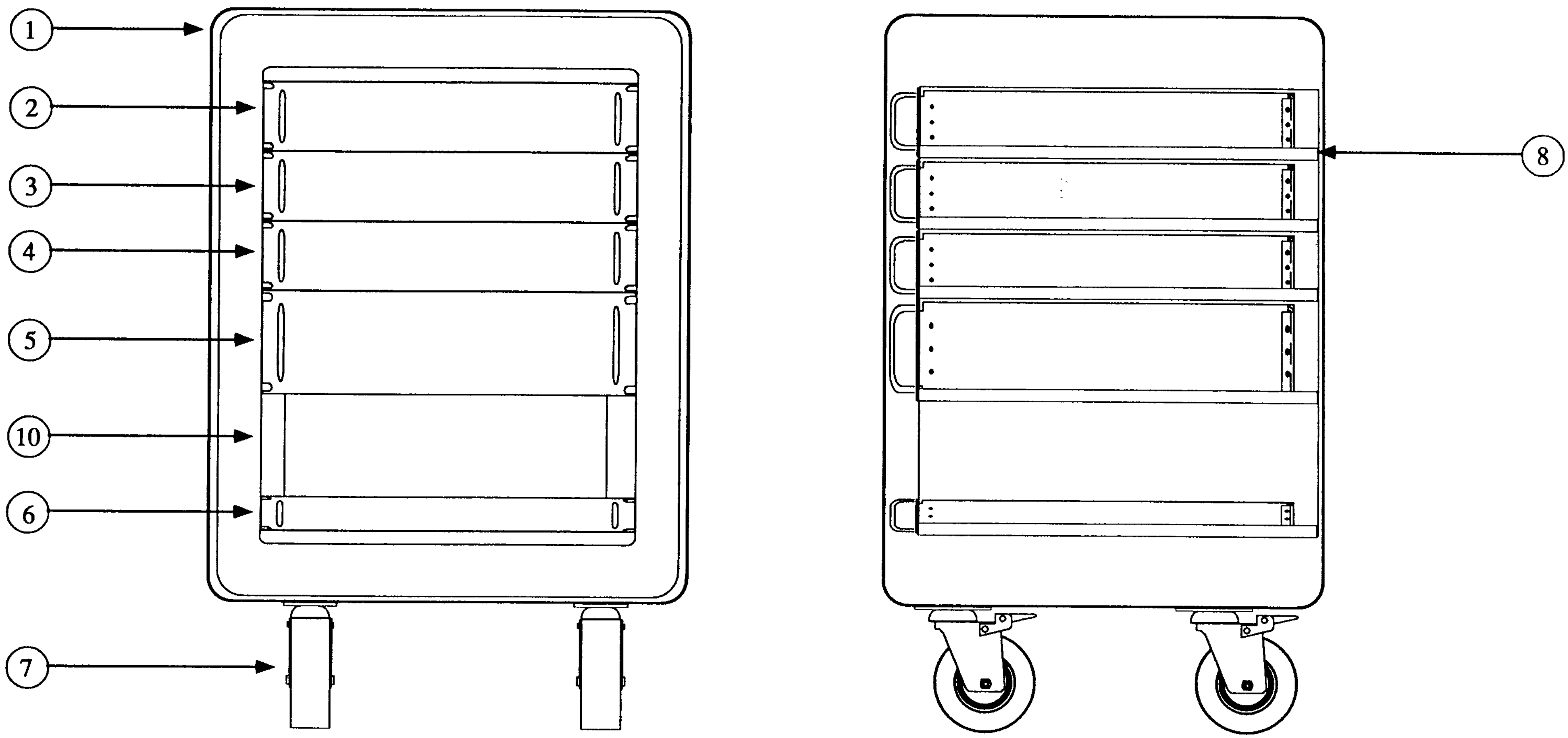

Fig. 2. HF Radar component chassis in shock mount container

Notes:

1. See ERIM document *TBD* for details concerning mounting chassis slides, cable routhing and associated hardware for the ECS enclosure.
2. This document incomplete without parts list 062-0005.

Space Physics Research Laboratory College of Engineering University of Michigan	Transceiver Assembly	REV		
		REV	04-29-96 NS	
		REV	04-26-96 NS	
		RELEASE		
N000149510249	Transceiver Assy	062- 0003	1 of 1	x2
		DRAWN	Neil Schnepf	
		COG ENG		

1 Drawing Page

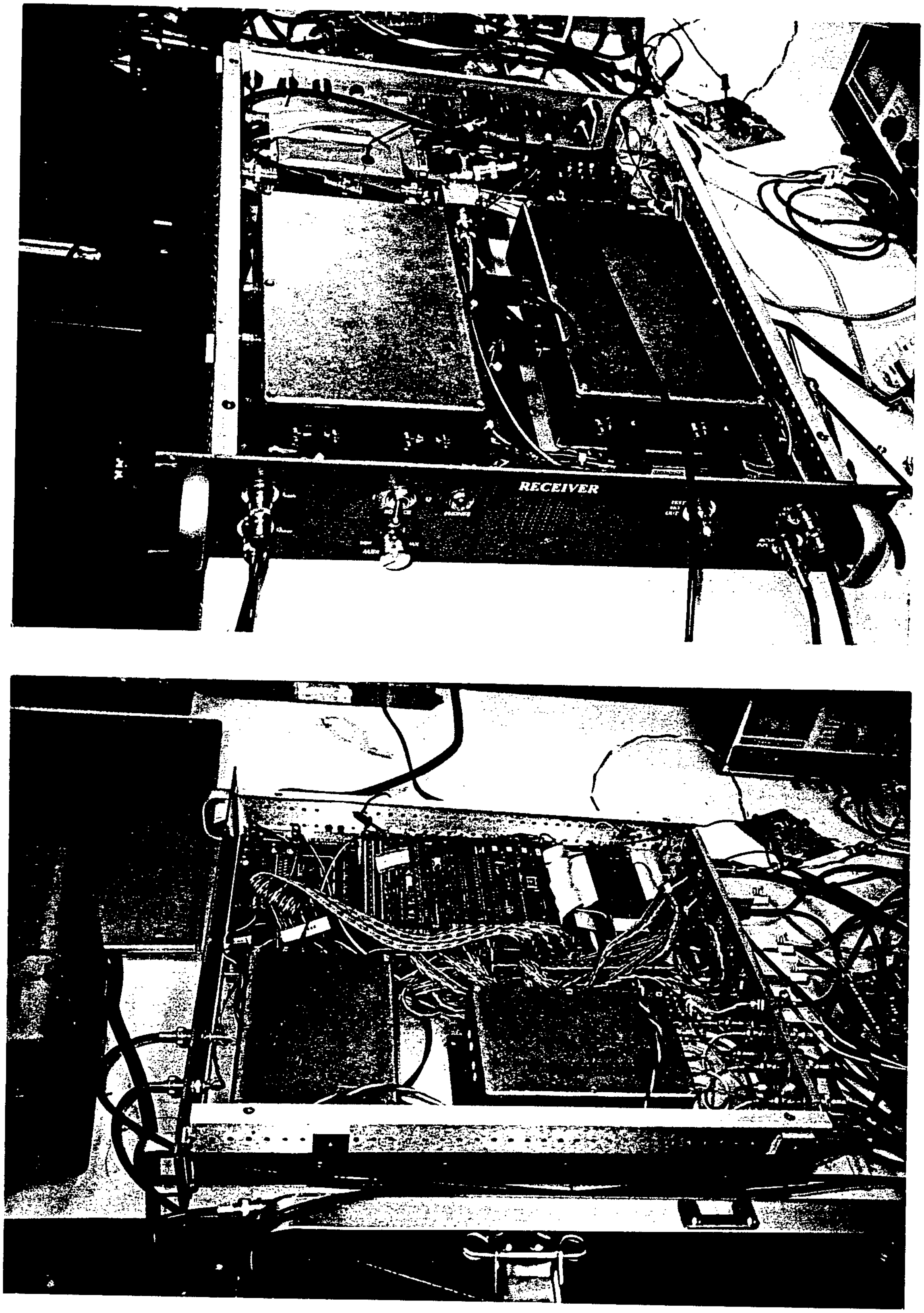

Fig. 3. Receiver (top) and controller-exciter (bottom) chassis with covers off during integration and test at the University of Michigan. Note that the receiver has a speaker so that one can listen to the received signals.

Photographs of the controller-exciter, receiver and transmitter chassis are shown in Figs 3 and 4.

An FCC license application was submitted in April, 1996 after consultation with FCC engineers and we anticipate that it will be granted without modification. It is very similar to license applications that were approved to operate radars along the California coast in the past.

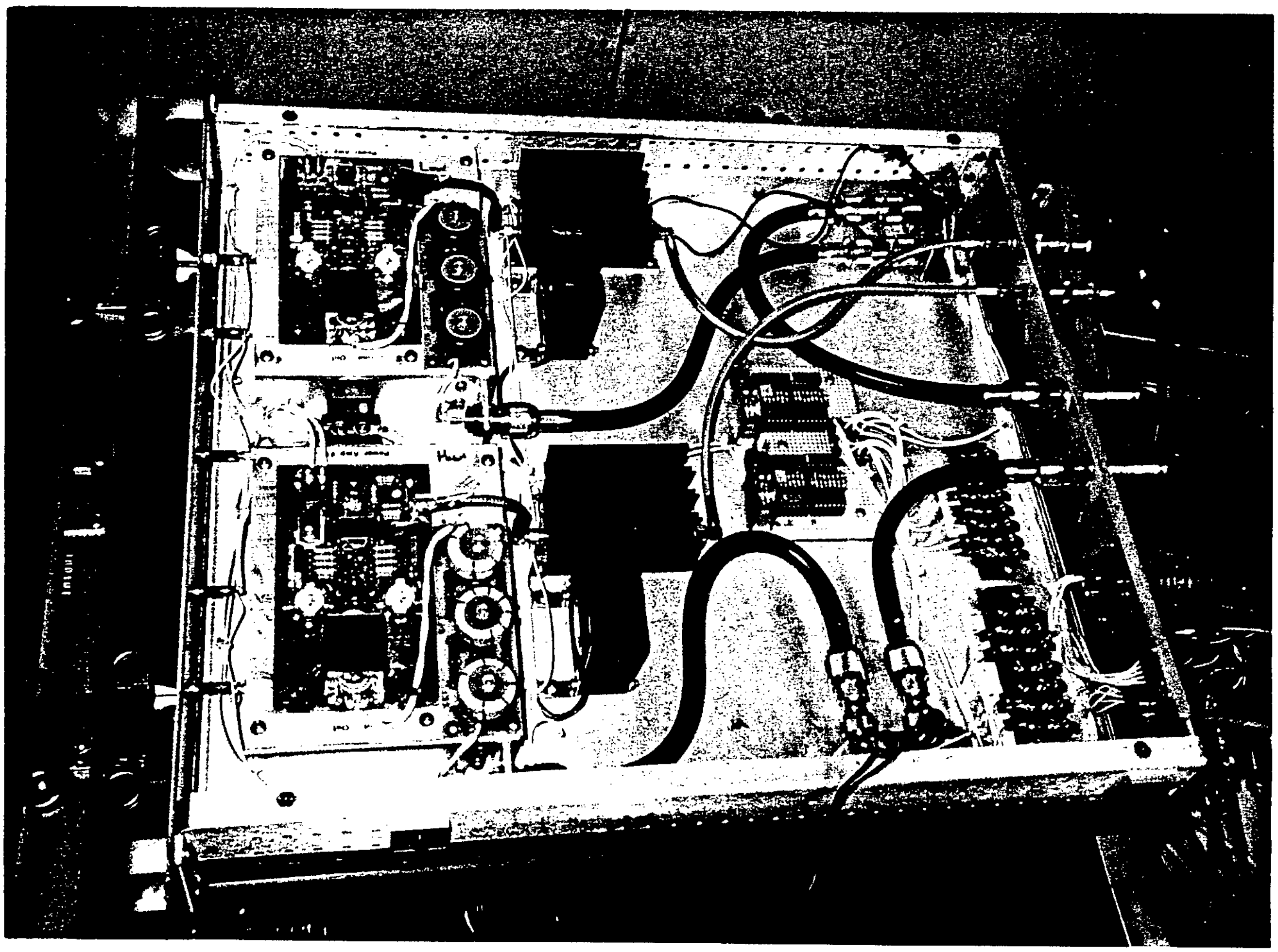

Fig. 4. Radar transmitter chassis during integration and test at the University of Michigan. The red upper and yellow (lower) inductors are part of the low pass filters for the transmitters.

III. Prototype Test Experiment Deployed at Long Marine Laboratory

Typical radar operation parameters are given in Table 1 below.

Table 1. HF Radar Operational Parameters

Radar frequencies	4.8, 6.8, 13.6 and 21.8 MHz
Radar wavelengths	62.5, 44.1, 22.1 and 13.8 m
Receiver antennas	8 element phased array of loops
Transmit antennas	two quarter wavelength verticals using traps to cover two frequencies with a single antenna
Peak power	50 to 100 W input to antenna feed
Range resolution	3 km with 50 kHz bandwidth
Angular resolution	15 to 67° depending on frequency
Maximum range	70 km depending on wave height/wind speed
Angular swath	± 60° from boresight
Sample duration	12 minutes
Sampling rate	up to 5 times per hour

The current location of the radar and coverage area are shown in Fig. 5. This site is kindly provided through collaboration with the REINAS project at UC Santa Cruz (Prof. Pat Mantey, director) and the Long Marine Laboratory of UC Santa Cruz (Steve Davenport, director). A second radar unit will be installed along the coast somewhere between Monterey and Elkhorn Slough, probably at the Moss Landing Marine Laboratory or near the former Ft. Ord beach front sites. In Fig. 6 we show the high band (13.6 and 21.8 MHz.) transmit antenna with the trap for two frequency operation near the upper guy rope connection.

Fig. 7 shows the receive antenna array with 8 elements space out over 50 m. This gives a spacing of half a wavelength at the highest frequency to reduce the effect of grating lobes in the antenna response. Each antenna has a separate preamplifier. The antennas are on a cliff overlooking the ocean at a height of about 15 meters above sea level. This is an ideal location for coupling surface wave energy into and out of the ground wave mode for propagation over the ocean.

Fig. 8 shows a close up of a receive antenna array element with high band antenna and guy ropes in the background. These square loops are about 2.5 ft. on a side and are made of 3/4 inch copper pipe. In Fig. 9 we show the 'trap' (consisting of a coil tuned, by the coaxial cable capacitor running down the left side of the pipe) that enables the high band antenna to operate on two frequencies. The transmit antennas are fed by RG-8U coaxial cable over a run of about 100 m from the transmitter. The receive antenna elements are connected to a multiplex box so that the receiver can be connected sequentially to each element of the antenna array.

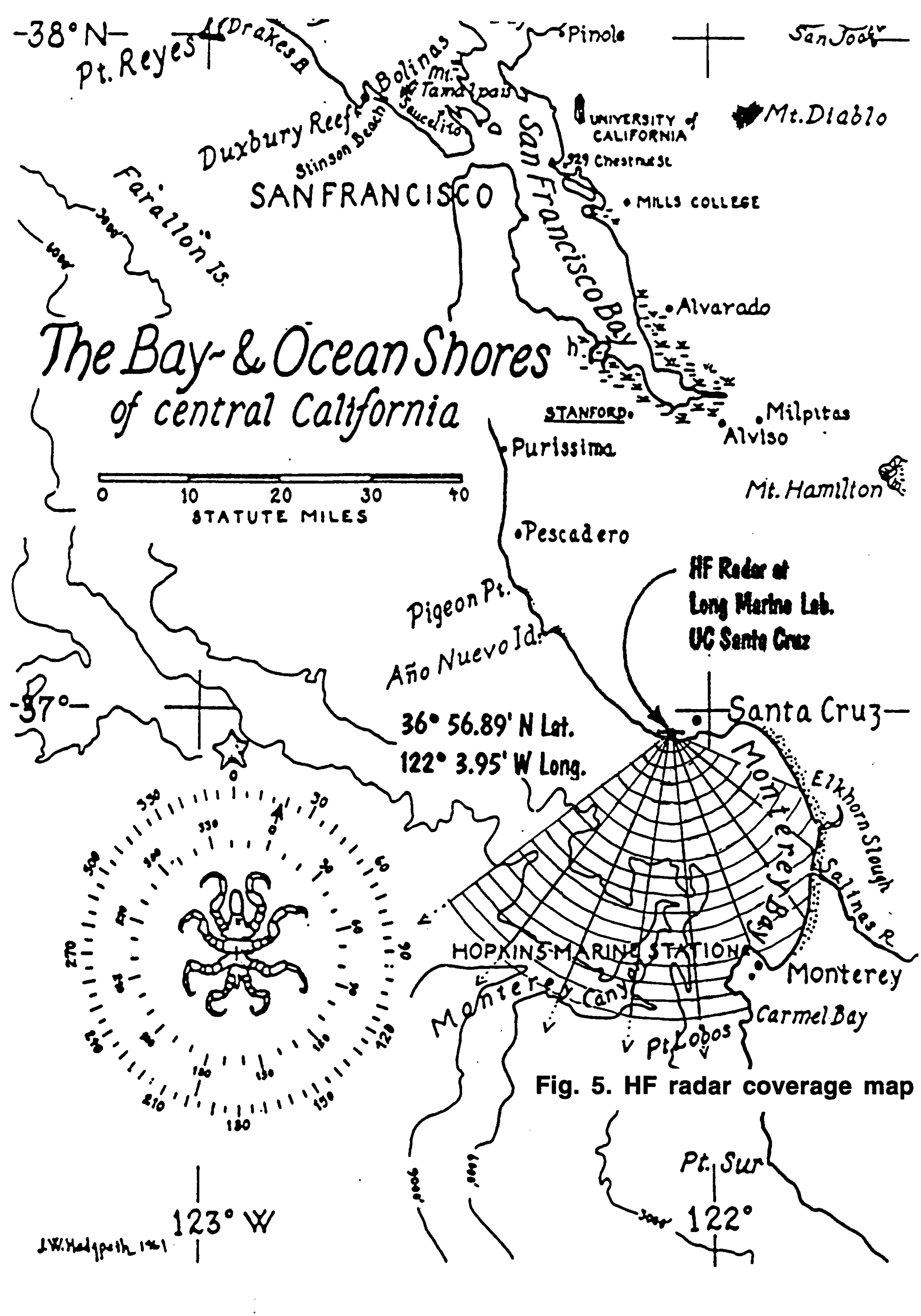

Fig. 5. HF radar coverage map

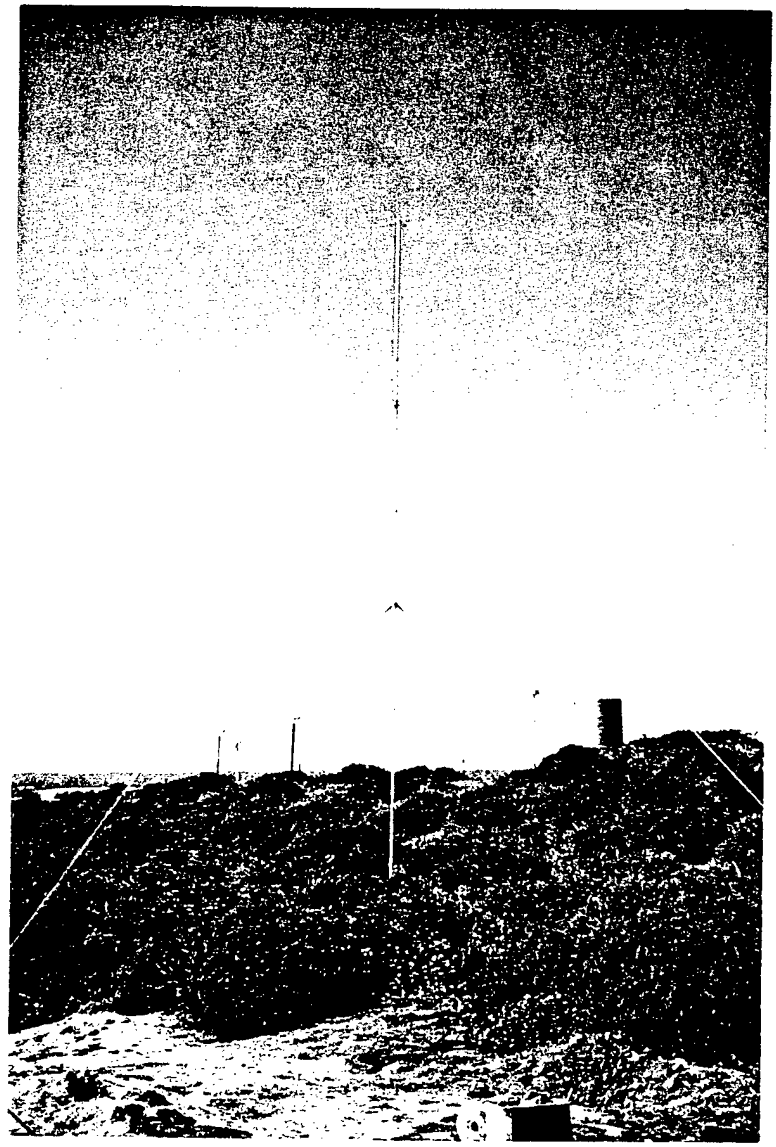

Fig. 6. High band transmit antenna. Note the 'trap' near the upper guy rope connection and the 'capacity hat' at the top to aid multifrequency operation. The antenna height is about 40 ft.

The primary output of the radar is the Doppler spectra of ocean echoes. This spectra is computed from a series of coherent samples taken over some 12 minutes. Thus, the spectral resolution is of the order of 1 to a few millihertz. Such high resolution is necessary to give accurate surface current estimates. An example, of spectra collected by the prototype radar is shown in Fig. 10. The transmit antennas used in this experiment have close to omni-directional patterns in the horizontal plane. The receive antennas have peak responses in directions perpendicular to the array long dimension, i.e. out toward the center of Monterey Bay (see Fig. 5) and in the opposite direction toward the Santa Cruz mountains. The prominent peak at zero Doppler in Fig. 10 is presumably due to land echoes from the back of the antenna array. The locations of the Bragg lines for 6.85 MHz are shown by the vertical dotted lines and the observed first-order Bragg lines are shown in both the lower and upper

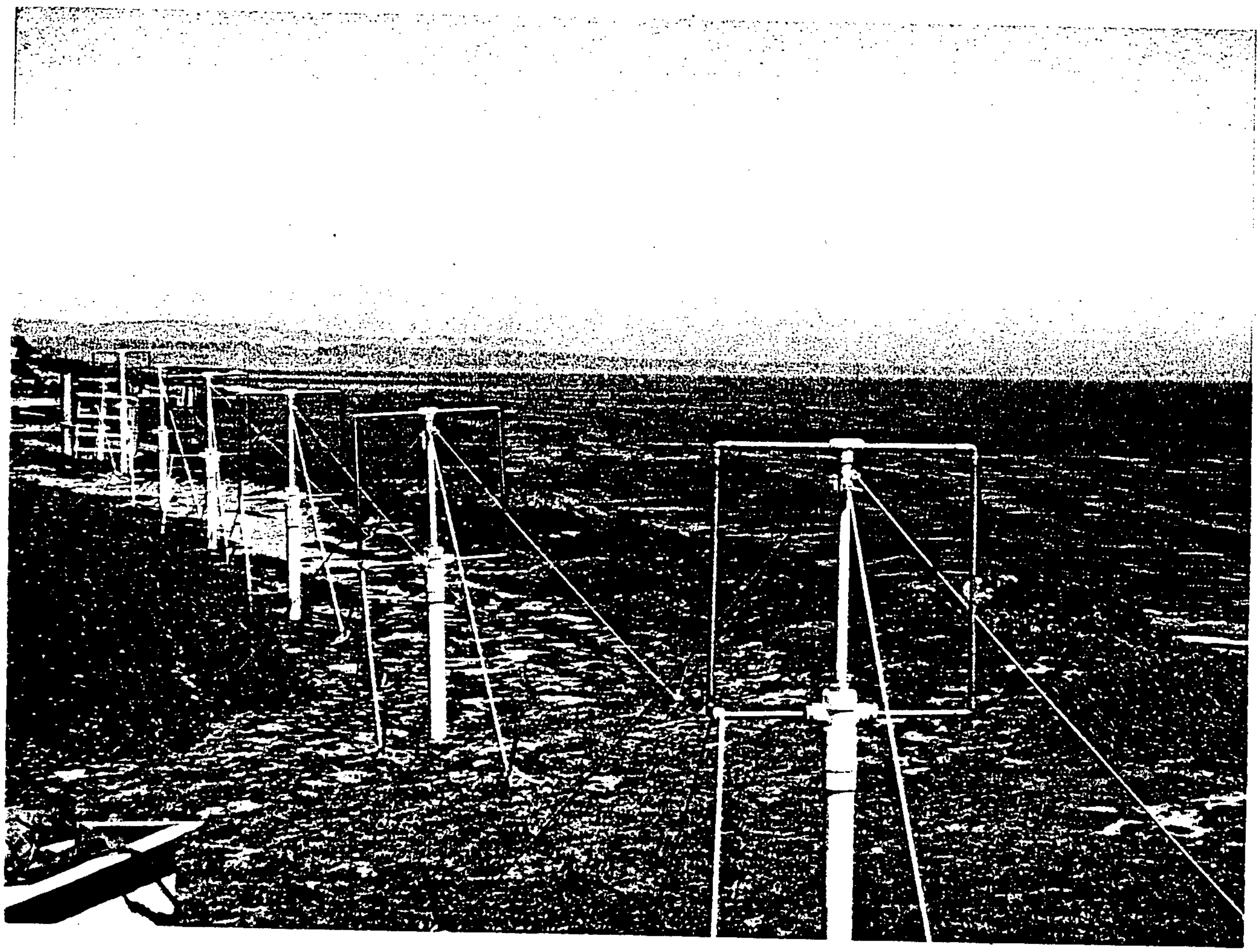

Fig. 7. HF antenna array on the north coast of Monterey Bay at the Long Marine Laboratory of the University of California at Santa Cruz.

panels. The negative Bragg peak is some 5 to 7 dB stronger than the positive peak since the prevailing wind (from the northwest on this particular day) is generating more receding (south traveling) waves than approaching (north traveling waves). Hence, in estimating currents we would use the displacement of the observed Bragg peak from the Bragg peak for still water (dotted line). So far we have simply used the highest SNR peak to make the current estimates. The horizontal lines near ± 0.6 Hz are fits to the spectral level and are used as the noise estimate in calculating SNR for the Bragg peaks.

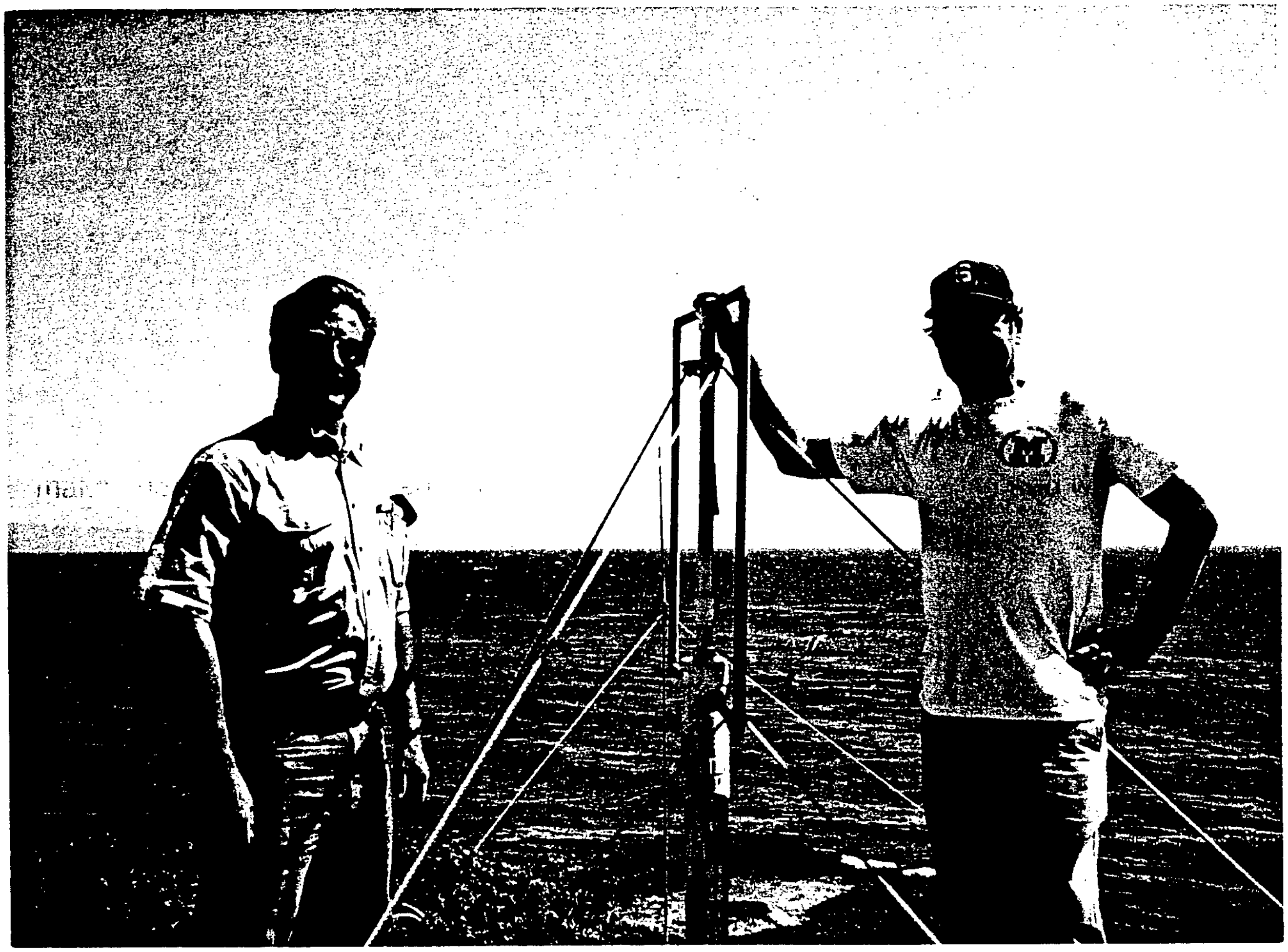

Fig. 8. Close up photo of a receive antenna element during the installation of the initial HF radar unit at Long Marine Laboratory of the University of California at Santa Cruz. Dr. Bob Onstott is on the left and Prof. John Vesecky on the right. The top of the antenna element is about 5.5 ft about the ground.

Before moving on to the initial results in terms of radial current maps we discuss a very necessary activity in effective HF radar operation, namely the use of a transponder to calibrated the amplitude and phase response of the antenna system. Assuming that all antenna elements are perfect is usually too great an assumption to make and leads to errors in the current estimates. Probably the most important effect is antenna pattern distortions and side lobes. These effects can lead to an ocean area with large currents 'leaking' into the estimates of areas with small currents and vice versa. Phase response variations across the receive antenna array can lead to faulty estimation of the spectra from which the current estimates are derived (see discussion above). To avoid these problems it is necessary to put a transponder at known

Fig. 9. Trap section of the high band HF antenna. The trap is about 3.5 meters off the ground and the total antenna height is about 5 meters.

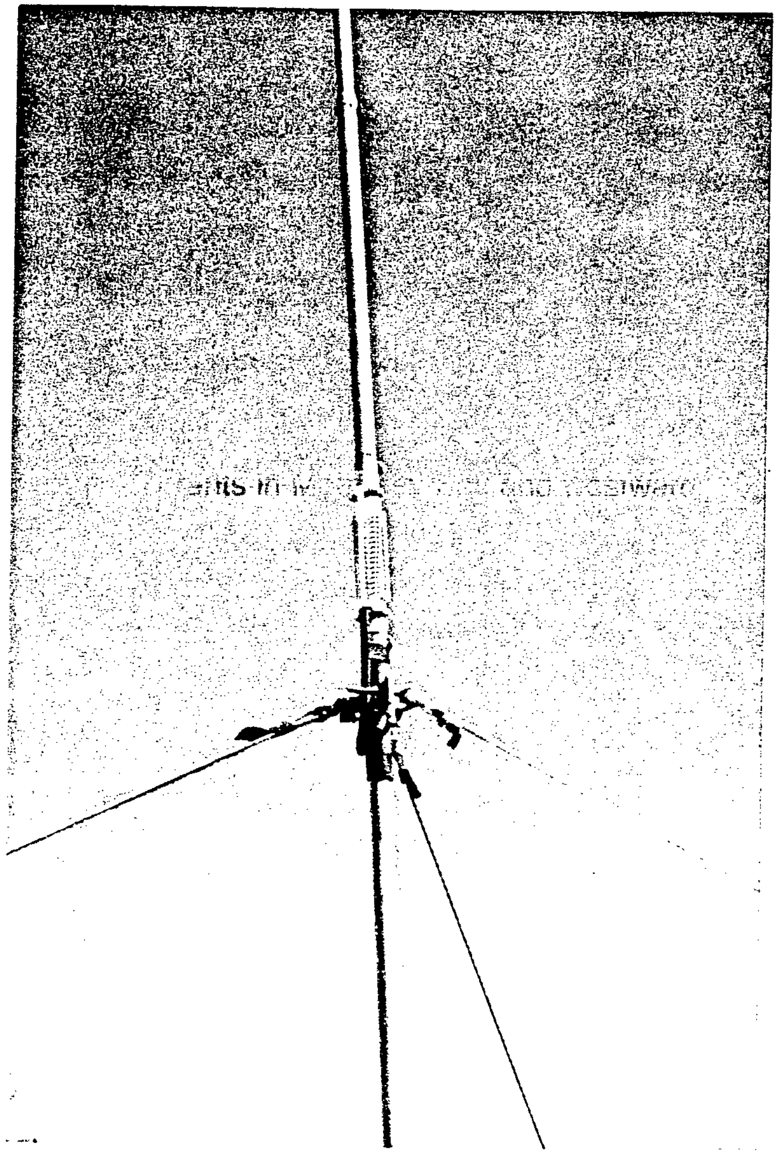

locations in the radar coverage area and collect radar echo data from the transponder to allow calibration of the antennas in terms of relative response in both phase and amplitude.

A transponder run was conducted on October 4, 1996 using a transponder constructed by the REINAS project at UC Santa Cruz (Dr. Dan Fernandez and Steve Petersen). Dr. Fernandez also acquired the cooperation of NOAA in providing the NOAA patrol boat, Sharkcat. The transponder was operated from about ten locations near the antenna site, but at different aspect angles relative to the antenna boresight. A sample transponder run spectrum is shown in Fig. 11.

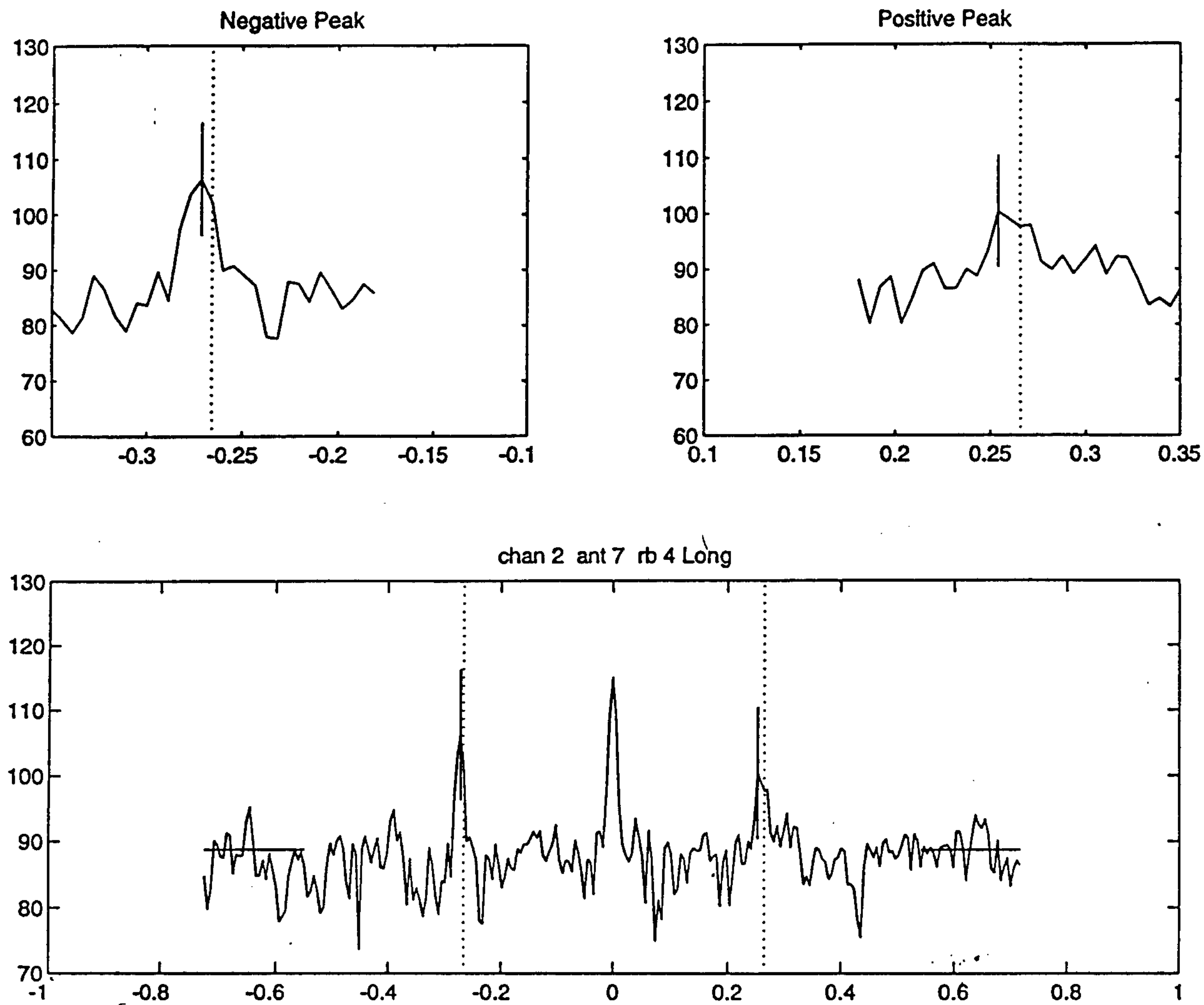

Fig. 10. Typical HF radar spectrum collected from a single antenna at the Long Marine Lab. site at a frequency of 6.85 MHz. Frequency scales are in Hz. The bottom panel shows the complete spectrum ± 0.7 Hz from the center frequency. The spectrum is for range bin 4 centered on a range of 12 km from the antenna site. The large peak at zero Doppler is presumably due to land echoes from the Santa Cruz mountains behind the radar site. The two spectral peaks, magnified in the upper panels, are from receding (negative peak) and approaching (positive peak) waves in Monterey Bay.

The transponder experiment of Oct. 4, 1996 was done in part because of the availability of the NOAA boat. The transponder was still in the prototype stage and had not been fully tested. The transponder worked, but the performance in terms of range was shorter than desired. The data are useful for a first-order current estimation algorithm, but better data quality from a higher power transponder output stage is needed. The transponder is now being modified to increase power and make other improvements. A new series of transponder runs will be done when the second unit is installed early in 1997.

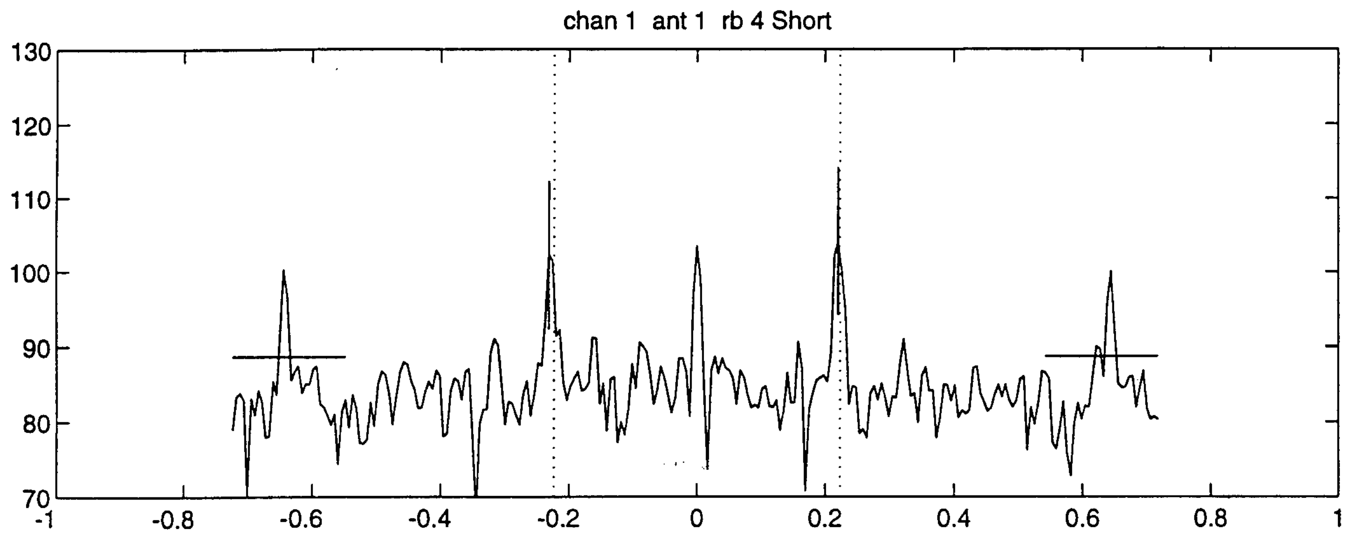

Fig. 11. Typical transponder run spectra. The spectral lines at ± 0.65 Hz are produced by the transponder and are analyzed to calibrate the antenna system in both phase and amplitude. The transmit frequency is 4.85 MHz and receiver antenna 1 was used for reception.

The beam forming algorithm and software development is in its early stages, but has produced initial results. At this stage the transponder data are good enough to allow for first-order phase and amplitude corrections. A prototype beam forming algorithm has been developed along straightforward lines. Matlab is being used as the prototyping software. Display software has also been created so that radial current profiles can be displayed in a geographical context.

Initial results for all four operating frequencies are shown in Fig. 12. These data were collected during the transponder run so we expect the phase and amplitude calibrations to be appropriate since there has been little time for antenna characteristics to change. The results are displayed on a range bin and angle bin grid with 3 km range bins and 15° angle bins. The 3 km range bins do not change with changes in operating frequency, but the angular resolution does change with frequency, increasing with decreasing frequency. Hence the 15° bins are not appropriate for the 4.8 MHz measurement where the angular resolution of the 50 m receive antenna array is only about 70°. Hence, in the 4.8 MHz results we find that the radial currents are very smooth with angle, extending over nearly the whole angular range. As operating frequency is increased, the variations with angle increase as the radars angular resolution is finer. Note also that the range of the radar is about 60 km in this instance. The range is influenced by the wind and may be reduced at low wind speeds.

Now consider the radial current maps in a geophysical context. We see that most of the measurements are receding, i.e. the radial current component is directly toward the south. This makes sense in that the prevailing winds are from the north. On the western side of the radar's coverage we find more variable currents. This also makes sense because it is in this region that there is often more current variability due to the interaction of the California current, flowing from north to south off the coast, with coast related currents influenced by the shore line and possible upwelling driven by winds out of the northwest.

As soon as we have thoroughly verified the beam forming and current estimation software, we plan to put the data products, e.g. Fig. 12, on the REINAS real time environmental measurement system. More useful measurements will be possible when two radars are installed and vector currents can be calculated. We propose to make such an installation and obtain vector currents in Monterey Bay and westward into the Pacific Ocean.

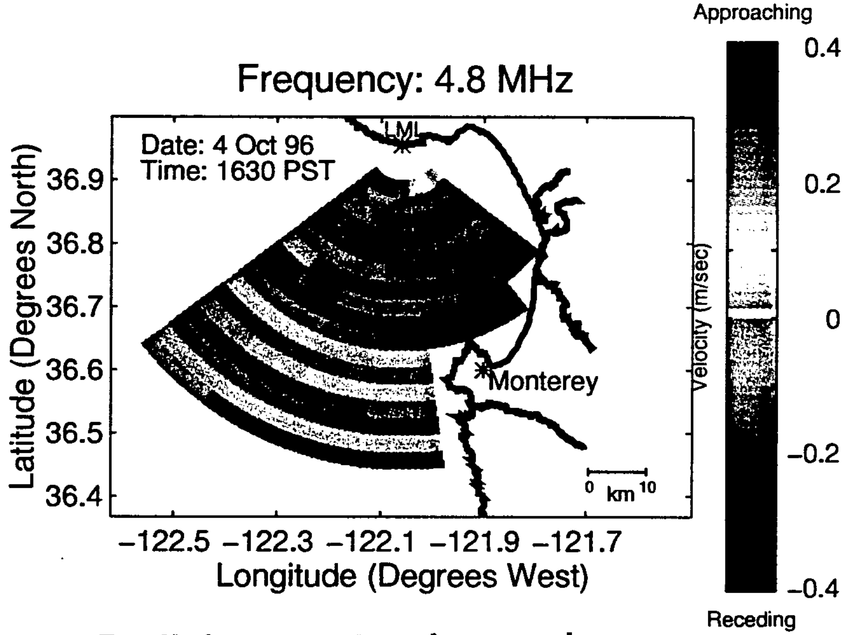

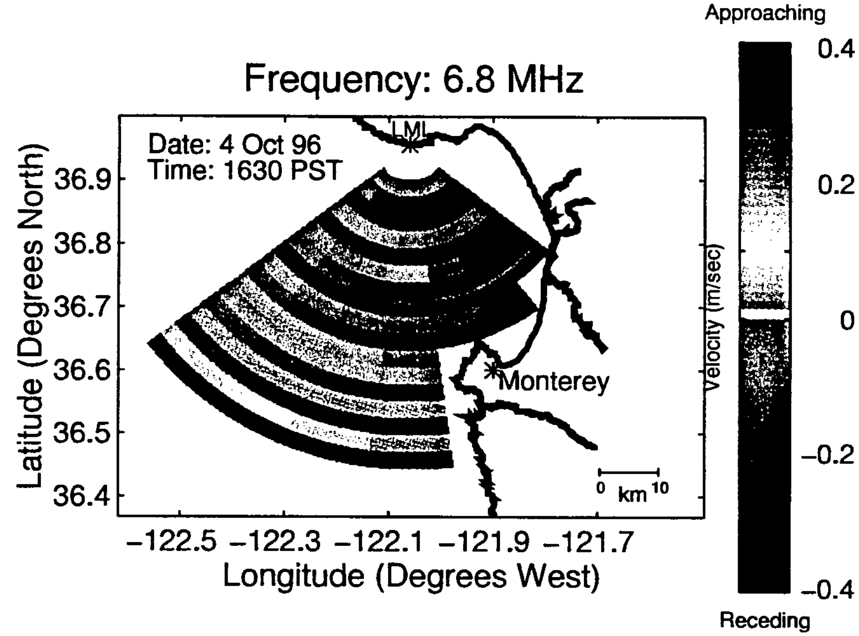

Fig. 12. Radial currents observed at four frequencies from the Long Marine Lab. site on the north shore of Monterey Bay

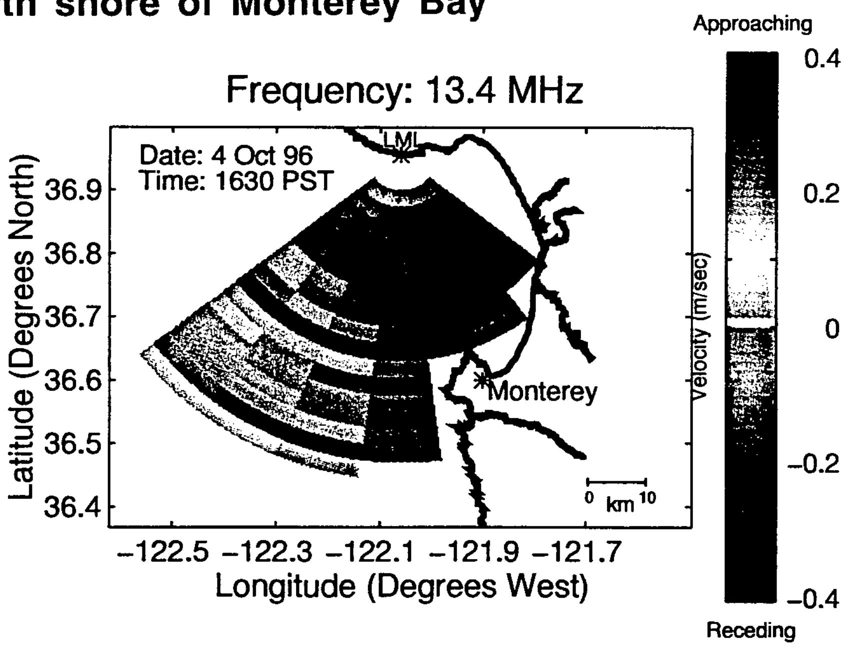

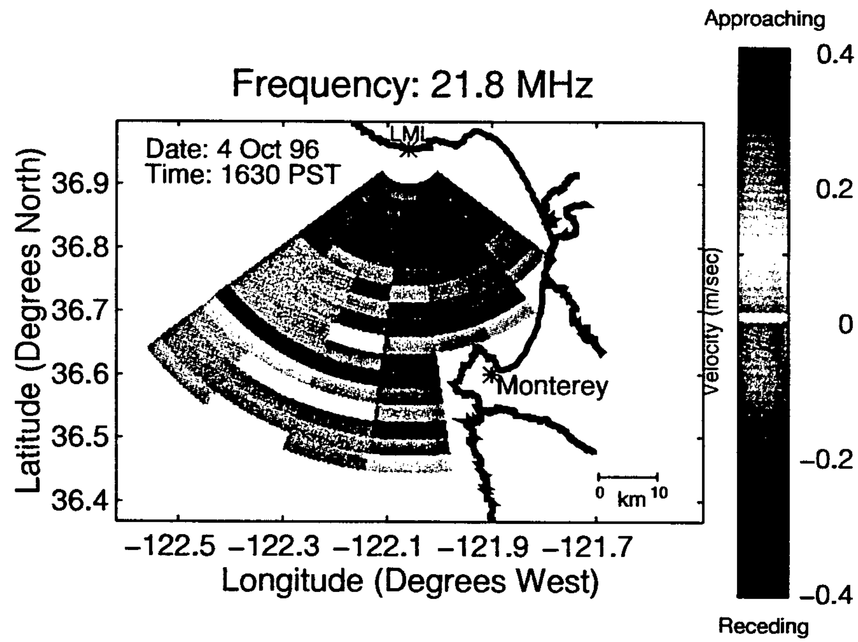

IV. Observations of Surface Current Vertical Shear

Observations of surface currents in Monterey Bay have revealed that although the currents at depths below 5 meters are primarily controlled by the tides and thus usually have a semi-diurnal (12 hour period) variation, the currents very near the surface are often controlled by local winds which often have a diurnal (24 hour period) due to the land-sea breeze effect. Observations our multifrequency HF radar unit at LML shows the transition between the wind forcing near the surface and the tidal forcing at deeper depths.

Since the radar observations of currents at different frequencies correspond to sensing different wavelength surface waves on the surface and since these waves 'feel' currents at different depths, HF radar observations at different frequencies correspond to the near surface current at different depths. For our HF radar the 'effective depths' of the four radar frequency channels are as follows:

Channel #	Radar Frequency -- MHz.	Resonant Ocean Wavelength -- m	Effective Depth -- m
1	4.8	31.3	1.6
2	6.8	22.0	0.9
3	13.6	11.0	0.5
4	21.8	6.7	0.3

Thus, observations at the four radar frequencies can give one a picture of the current behavior at several depths in the top two meters of the ocean. To illustrate the usefulness of this capability we examined the current variations at two observational frequencies as functions of location and time over a 24 hour period. However, before examining the radar data we describe the wind variations over this period. Fig. 13 shows the wind speed variation at the location of the M1 buoy deployed by the Monterey Bay Aquarium Research Institute and kindly provided via their internet homepage. These data were collected on October 17, 1996 at a location approximately midway between the LML radar site and the Monterey Peninsula shown in Fig. 5 above. Thus, this buoy lies very close to the broadside direction of our HF radar antenna. Fig. 14 shows the wind direction from the M1 buoy. The low winds from the NE in the morning hours, followed by much stronger winds from the NW in the afternoon and early evening hours are typical of the wind fluctuations over Monterey Bay in the spring, summer and autumn. In Fig. 15 we show the tidal height at Moss Landing, on the coast near the middle of Monterey Bay. It shows the typical semi-diurnal variation of the tides in Monterey Bay.

In Figs. 16 and 17 we show HF radar derived, radial currents that correspond to a radial cut in the plots of Fig. 12 as a function of time. The cut displayed in Figs. 16 and 17 is broadside to the antenna array direction and on a bearing of 171° T. These data have been smoothed and correspond to a broad swath across the mouth of Monterey Bay from the LML site southward toward the Monterey Peninsula as shown in Figs. 5 and 12. The range bins correspond to increments of 3 km in range with the middle of Monterey Bay corresponding to about range bin

10 on the plots. In Fig. 16 we show the radial currents from Channel 4 with an effective depth of about 30 cm. They show a strong diurnal variation as also observed by Paduan et al. (1995) in August of 1994, at an effective depth of about 30 cm, about the same as that of our Fig. 16. Here we are able to observe currents deeper below the surface and the results for an effective depth of about 1 meter are shown in Fig. 17. Here, we can see the struggle between the diurnal forcing of the wind and the semi-diurnal forcing of the tides. Near the middle of the bay, range bin 10, we see a clear semi-diurnal variation. We suspect that this variation corresponds to the domination of the tides at a depth of about one meter.

Clearly these are only preliminary results and just for a single day. Yet they clearly indicate a transition from diurnal to semi-diurnal behavior with increasing depth. More careful study, including a second radar unit and use of current measurements from the acoustic Doppler current profiler (ADCP) associated with the M1 buoy, will commence in early 1997.

References

Paduan, J. D., E. T. Petruncio, D. E. Barrick and B. J. Lipa, Surface currents within and offshore of Monterey Bay as mapped by a multiple-site HF radar (CODAR) network, Proceedings of the 5th IEEE Working Conference on Current Measurement, St. Petersburg FL, 7-9 February (1995)

JFV 2/8/97

Fig. 13. Marine wind speeds observed by the M1 buoy deployed near the center of the mouth of Monterey Bay. The times are local time on 10/17/96. Note the diurnal land-sea breeze variation.

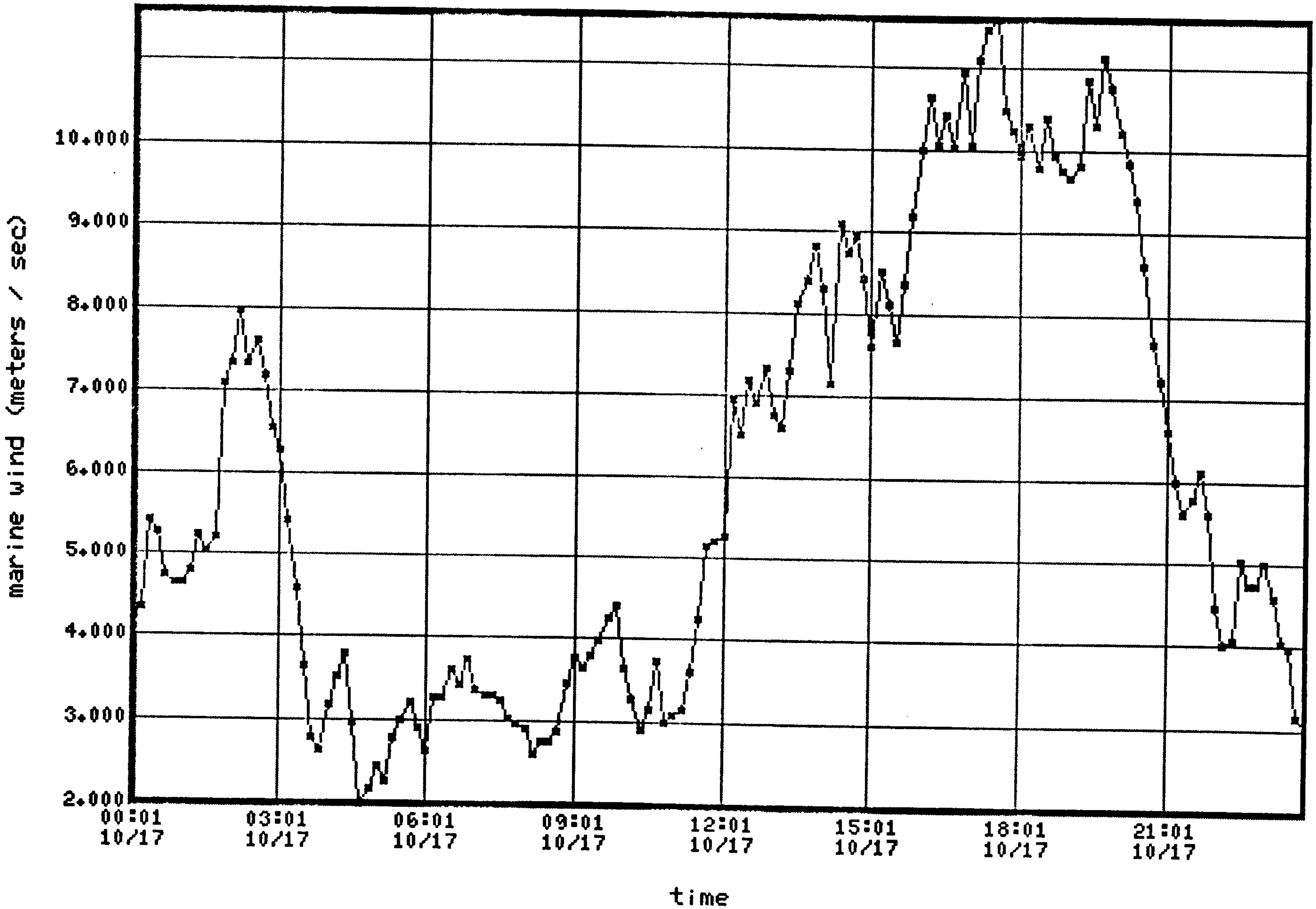

Fig. 14. Marine wind directions observed by the M1 buoy deployed near the center of the mouth of Monterey Bay. Note that the directions are those toward which the wind blows. The times are local time on 10/17/96.

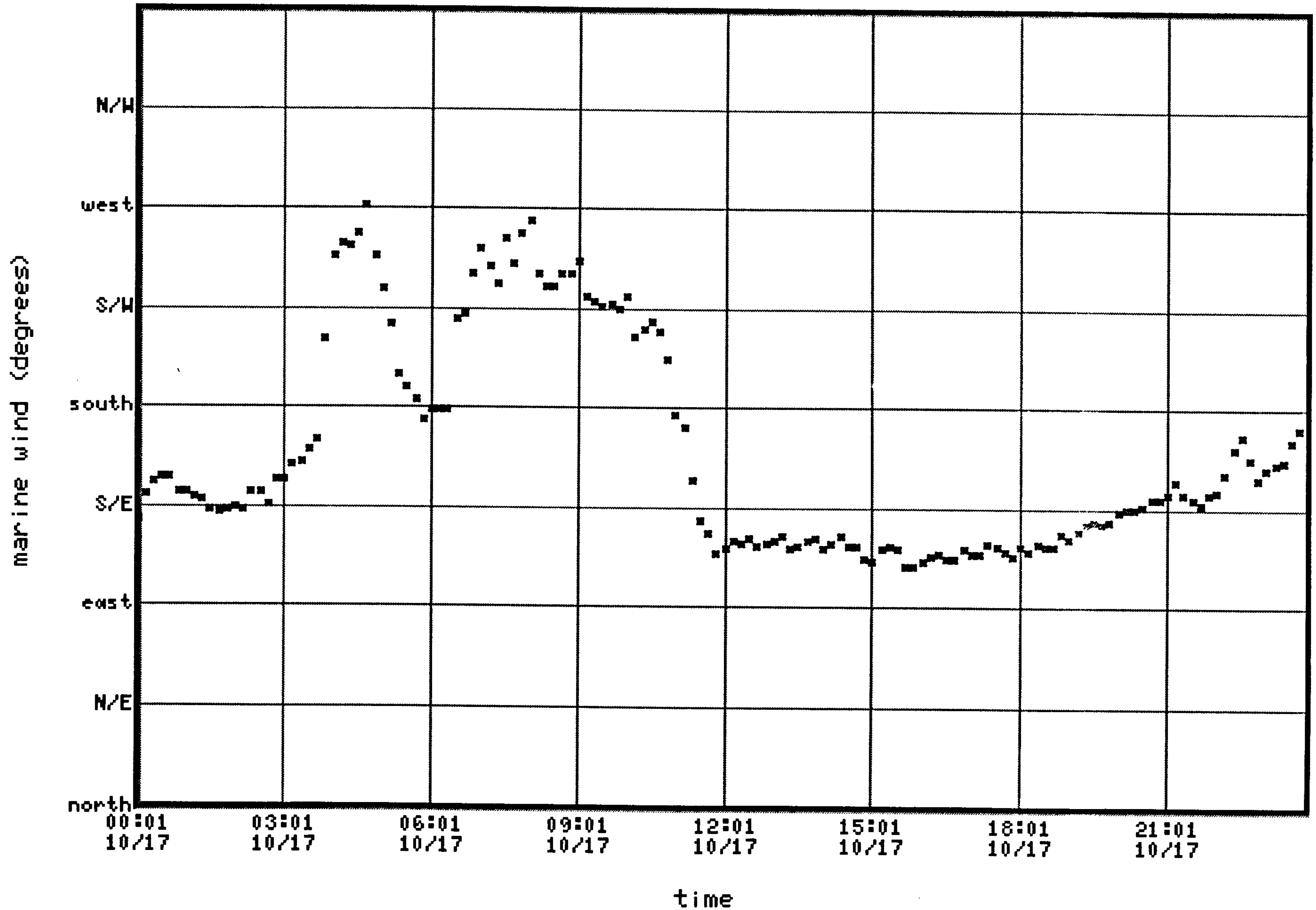

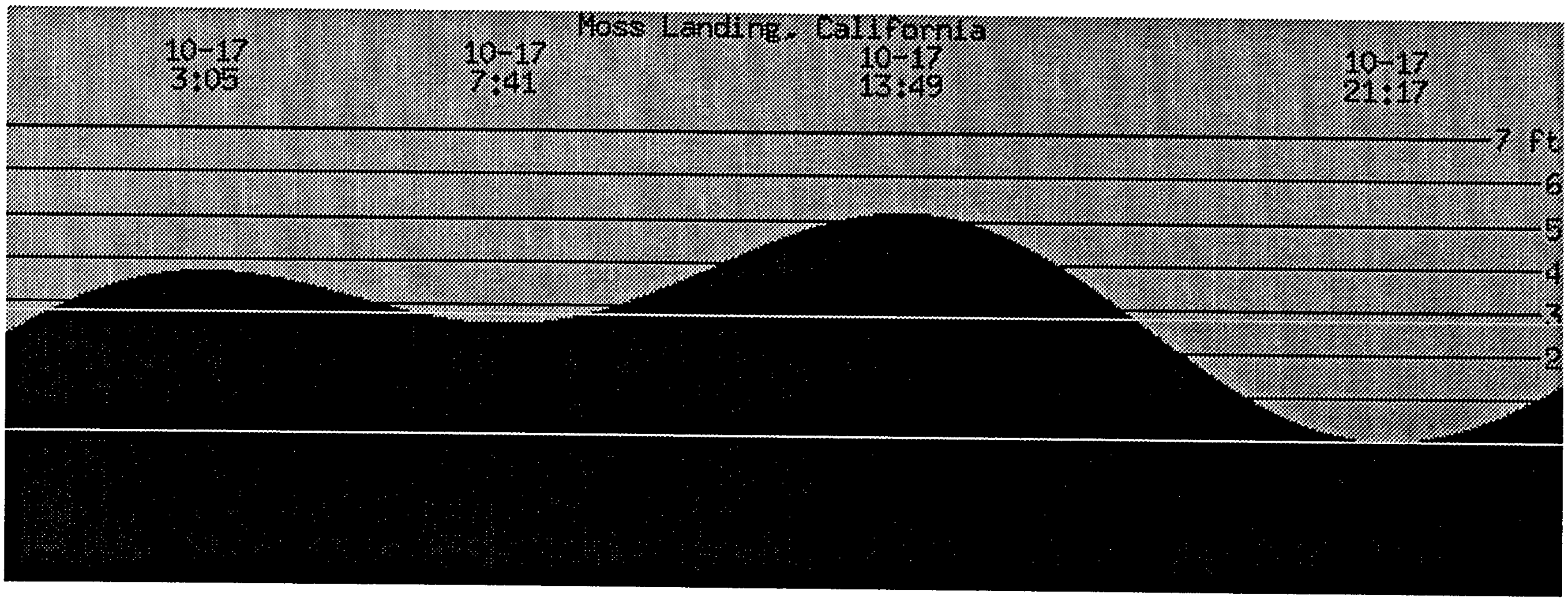

Fig. 15. Tidal height observed at the Moss Landing Marine station on the coast near the center of Monterey Bay. The times are local time on 10/17/96.

Change of Ocean Current Over Time

Channel 4, Broadside
October 17, 1996

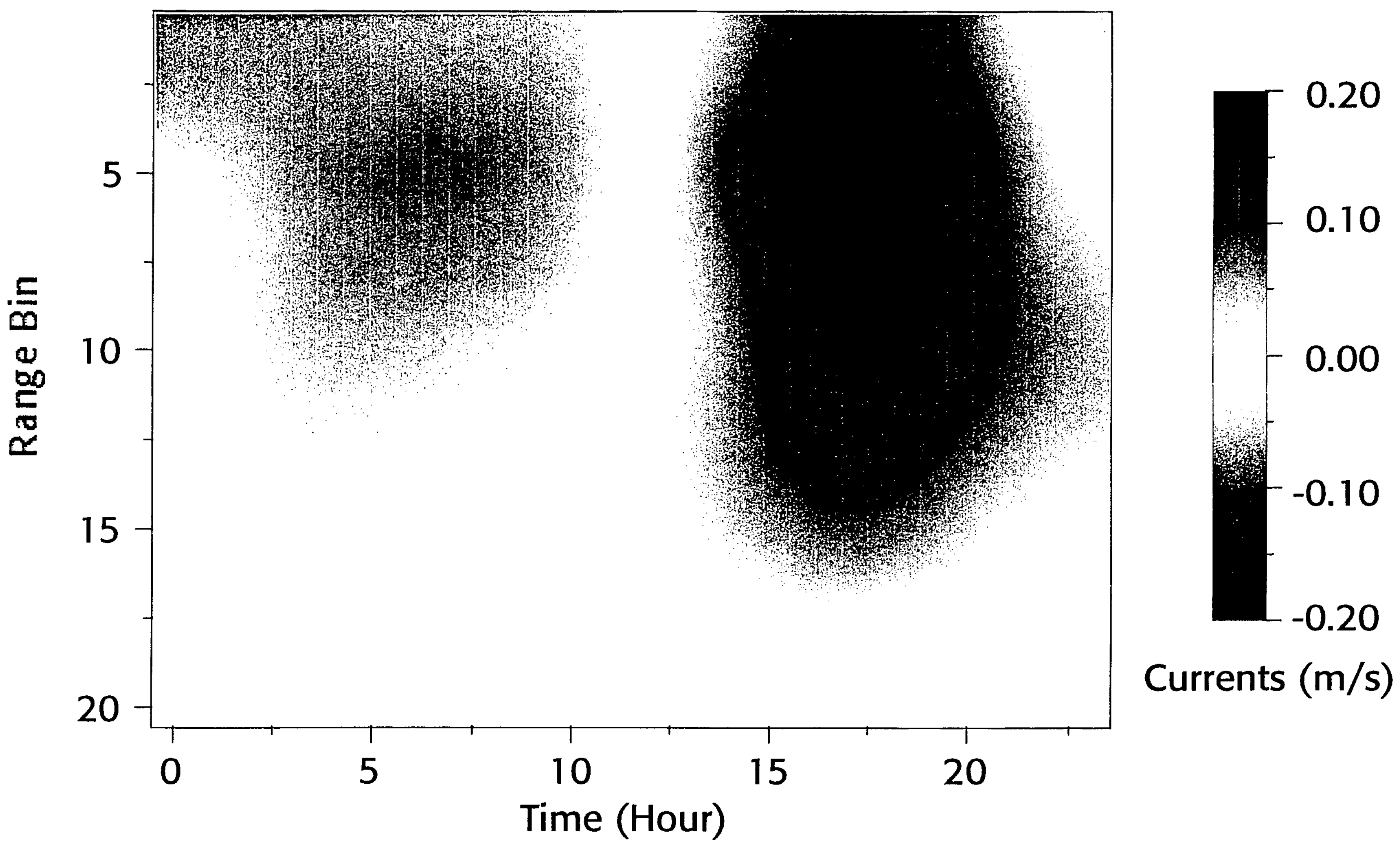

Fig. 16. Radial currents observed by HF radar channel 4 with an effective depth of about 30 cm. Times are local time. Note the strong diurnal variation.

Change of Ocean Current Over Time
Channel 2, Broadside
October 17, 1996

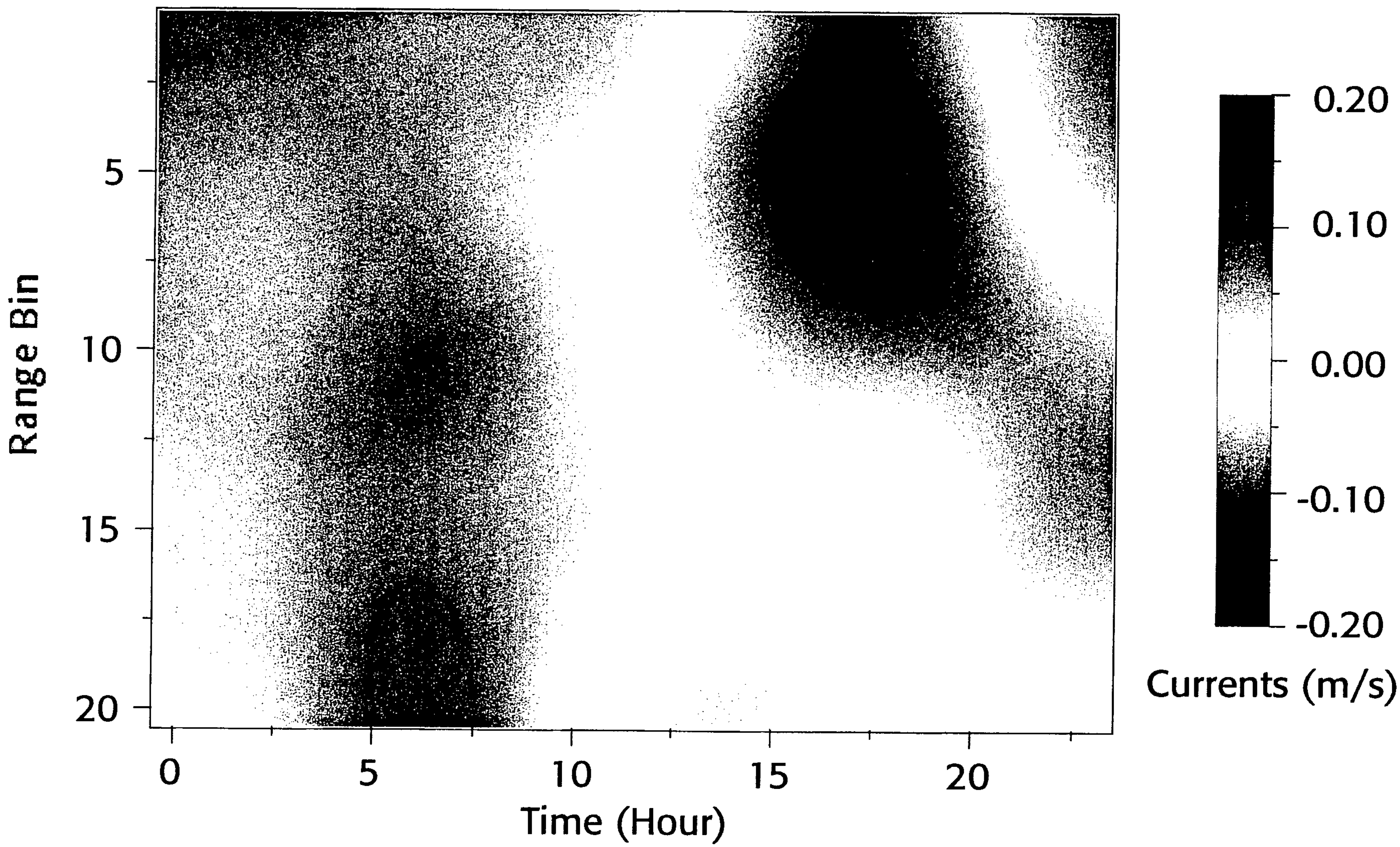

Fig. 17. Radial currents observed by HF radar channel 2 with an effective depth of about 90 cm. Times are local time. Note the combination of diurnal and semi-diurnal variations.